Observation of a Shape Resonance in Cold-Atom Scattering by Pulsed Photoassociation

H. M. J. M. Boesten,[1] C. C. Tsai,[2] B. J. Verhaar,[1] and D. J. Heinzen[2]
[1]*Eindhoven University, Box 513, 5600MB Eindhoven, The Netherlands*
[2]*Department of Physics, The University of Texas, Austin, Texas 78712*
(Received 12 July 1996; revised manuscript received 27 September 1996)

We observe the time dependence of a cold-atom collision in a pulsed photoassociation experiment. For a g-wave shape resonance in the ^{85}Rb + ^{85}Rb system we measure the time needed to build up the resonant state by tunneling through the centrifugal barrier. Combining this with time-independent ^{85}Rb and ^{87}Rb photoassociation we determine the resonance energy and find evidence for the decay of the shape resonance into inelastic channels. We also determine the ^{85}Rb + ^{85}Rb and ^{87}Rb + ^{87}Rb C_6 coefficient and triplet scattering lengths without relying on *ab initio* calculations. [S0031-9007(96)01931-X]

PACS numbers: 34.50.Rk, 32.80.Pj, 33.70.Ca

Recent developments in laser cooling and evaporative cooling techniques, especially for alkali gas samples, have led to the rapidly expanding field of cold collision physics. Collisions between cold atoms are exceptional in a number of aspects. One of these is the frequent occurrence of shape resonances, which are elastic scattering resonances associated with quasibound diatomic levels trapped behind a centrifugal barrier. These are important to the collision physics because the collision energies are typically lower than the centrifugal barrier even for the lowest nonvanishing l partial waves. Considering the vibrational and rotational energy spacings of the alkali dimers, the probability for any of these to have at least one quasibound state with $l \leq 6$ is more than 50%. Knowing the energy of a shape resonance leads very directly to an accurate scattering length for the corresponding potential and is nearly equivalent to finding the last bound state of that potential. Shape resonances may be expected to create possibilities for many exciting new experiments. In particular, they will shed new light on the elastic and inelastic interactions of cold atoms, which are of crucial importance for understanding Bose-Einstein condensation phenomena [1–3], laser-cooled atomic clocks [4], and other cold-atom applications. They may also lead to a new kind of spectroscopy of states inside the centrifugal barrier with a tunneling lifetime long enough for inelastic interactions to occur due to weak interaction terms that are difficult to study otherwise.

In this Letter, we present the first detailed study of a shape resonance in cold atomic scattering, focusing our attention on a g-wave resonance in the scattering of two ^{85}Rb atoms. We observe this resonance with cold-atom photoassociation [5–10]. Photoassociation is particularly useful for the present study, since it allows us to excite atomic pairs in a narrow radial range around $40a_0$ that is inside the centrifugal barrier at about $100a_0$, and also because it allows us to probe individual partial wave components of the collision [10]. That is, we can selectively photoexcite the collision resonance.

The ^{85}Rb + ^{85}Rb g-wave shape resonance is sufficiently long lived that we are also able, for the first time, to directly observe time dependence in cold atomic collisions. With a pulsed photoassociation experiment, we measure the buildup of the resonance state by tunneling through the barrier in competition with various decay processes. The lifetime of the shape resonance is also long enough to be comparable to the time scale for inelastic interaction processes in the scattering of Rb ground state atoms. In agreement with this the time-independent photoassociation spectrum associated with the excitation of a $J = 4$ excited rotational state shows anomalous features that cannot be reproduced in terms of elastic scattering alone. The anomalous features can be explained in terms of an additional broadening of the resonance due to inelastic decay channels.

As in our previous experiments [5,6,10], we illuminate trapped, laser-cooled, doubly spin-polarized Rb atoms with light from a tunable photoassociation (PA) probe laser, and detect the absorption of this light by colliding pairs of atoms with a trap-loss method. To begin each measurement, we load about 10^4 ^{85}Rb atoms from a vapor-cell magneto-optical trap into a far-off-resonance optical trap (FORT) with a waist of about 10 μm and depth 10 mK. Subsequently, for 200 ms the atoms are illuminated by a combination of laser fields. Each 200 ms period consists of repeated 5 μs cycles, as shown in Fig. 1(a). For the first 2.5 μs, only the FORT laser beam is on. For the next 2.2 μs, the atoms are illuminated by light from the tunable PA laser, and for the last 0.3 μs, the atoms are illuminated by a pair of optical pumping beams. (We also sometimes use repeated 10 μs cycles, for which the PA laser period is 4.7 μs.) The combination of the FORT and optical pumping light keeps the atoms trapped and in their doubly-spin polarized $|F = 3, M_F = 3\rangle$ state, in a manner exactly analogous to that described in Ref. [10]. At the end of each 200 ms period, the atoms are probed with laser-induced fluorescence (LIF), the intensity of which is proportional to the number of

 0031-9007/96/77(26)/5194(4)$10.00

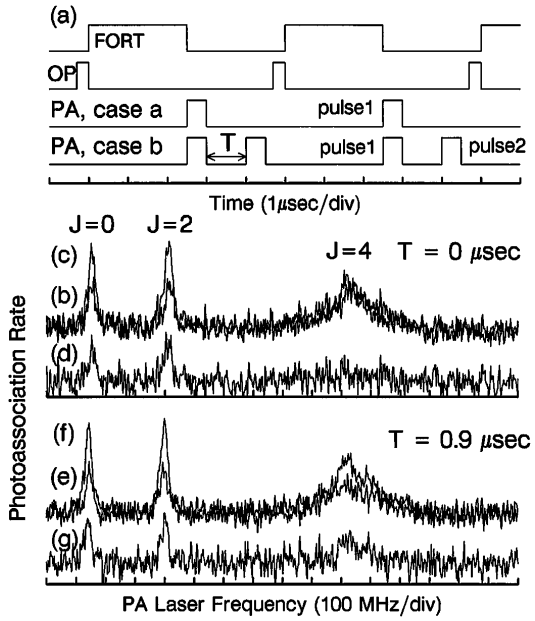

FIG. 1. (a) Timing of laser pulses in the experiment. (b)–(g) Time-dependent photoassociation spectra of the 0_g^- vibrational level at 12 573.04 cm^{-1} (loss rate is plotted downward). (b),(e) Spectrum with one photoassociation pulse only. (c),(f) Spectrum with two photoassociation pulses. (d),(g) Difference spectra showing the effect of pulse 2 alone. (b)–(d) $T = 0$. (e)–(g) $T = 0.9$ μs. Notice that, for $T = 0$, in contrast to the $J = 0$ and $J = 2$ lines, the $J = 4$ peak is not twice as high in spectrum (b) in comparison with spectrum (a). But, when pulse 2 is delayed as in trace (f), an additional signal appears in the $J = 4$ peak.

atoms remaining in the trap. If the PA laser induces free-bound optical transitions, the LIF signal is reduced, because any atoms which are excited decay predominantly to free atomic states which are too energetic to remain in the FORT. These steps are repeated for a succession of PA laser frequencies.

In order to directly probe the time dependence of these collisions, we further subdivided the 2.2 μs (or 4.7 μs) periods into a pulse sequence [Fig. 1(a)] consisting of either a single 0.45 μs duration pulse (pulse 1) (case a), or a 0.45 μs duration pulse (pulse 1) followed by a variable time T, and then followed by a second 0.45 μs duration pulse (pulse 2) (case b). We tuned the PA laser over the $|^{85}\mathrm{Rb}\ (5^2S_{1/2}F = 3, M_F = 3) + {}^{85}\mathrm{Rb}\ (5^2S_{1/2}F = 3, M_F = 3); \epsilon, l, m_l, \rangle \rightarrow |^{85}\mathrm{Rb}_2(0_g^- \sim 5^2S_{1/2} + 5^2P_{1/2})v, J\rangle$ transitions, where ϵ, l, and m_l denote the energy and orbital angular momentum quantum numbers of the initially free state. We probed all the rotational levels J belonging to the vibrational level v which lies at an energy of -3.365 cm^{-1} with respect to the barycenter of the $5^2S_{1/2} + 5^2P_{1/2}$ dissociation limit. A typical result, recorded at a PA laser intensity of 57 W/cm^2, is shown in Fig. 1. Figures 1(b)–1(d) show the result when the delay time T was set to zero, and Figs. 1(e)–1(g) show the result when the delay time was set to 0.9 μs. Figures 1(b) and 1(e) show the result for case a (pulse 1 only), Figs. 1(c) and 1(f) show the result for case b (pulse 1 and pulse 2), and Figs. 1(d) and 1(g) show the difference between case b and case a. The difference shown in Figs. 1(d) and 1(g) represents the signal due to pulse 2 alone, i.e., the increased trap loss due to the formation and optical excitation of new g-wave states.

Each spectrum consists of three lines, which correspond to the $J = 0$, 2, and 4 rotational levels. As has been discussed previously [10], for the particular transition we have chosen an electronically excited state with a Hund's case (e) structure [11], the selection rule $J = l$ is obeyed. Thus, the $J = 0$ peak arises from the s-wave part of the scattering wave function, the $J = 2$ peak from the d-wave part, and the $J = 4$ feature from the g-wave part. The odd rotational peaks are suppressed because the spin-polarized Rb atoms are identical bosons and therefore cannot exist in odd partial wave states. The $J = 4$ peak saturates at an intensity of 0.5 W/cm^2, which is much less than the intensity of 15 W/cm^2 at which the $J = 0$ and $J = 2$ peaks saturate. This causes the $J = 4$ peak to be power broadened when the $J = 0$ and $J = 2$ peaks are visible (Fig. 1). The greatly reduced saturation intensity of the $J = 4$ peak occurs because the g-wave shape resonance increases the g-wave vibrational wave function amplitude and therefore increases its optical transition strength.

The lifetime of this resonance is long enough that we are able to see it directly in the data of Fig. 1. For a very rapid collision time scale, the signal should be proportional to the total time the PA laser is on. This occurs for the $J = 0$ and 2 peaks, where the height of the peaks for case b (total PA on time/cycle = 0.9 μs) is about twice that for case a (total PA on time/cycle = 0.45 μs). However, a completely different behavior is observed for the $J = 4$ peak. For no delay time [Figs. 1(b)–1(d)] pulse 2 induces much less signal than pulse 1. This occurs because pulse 1 is sufficiently intense to remove all pairs of atoms in the g-wave resonant state from the trap. Since it takes time for new atoms to tunnel through the g-wave centrifugal barrier, pulse 2 finds very few pairs of g-wave atoms at $\sim 40a_0$ separation. On the other hand, when the delay time is increased, as in Figs. 1(e)–1(g), pulse 2 induces a significant additional signal. This occurs because the delay time is comparable to the tunneling time, so that new g-wave resonant states are formed and optically excited by the second pulse.

Three mechanisms compete in depleting the resonant amplitude built up by inward tunneling (rate γ_{in}): tunneling outward through the barrier (γ_{out}), photoassociation to a bound excited state (γ_L), and inelastic decay to lower ground-state hyperfine levels (γ_{inel}). We have carried out a combined analysis of both the time-dependent data and a time-independent spectrum of the same levels. The time-dependent data are sensitive mostly to the total resonance

decay rate $\gamma_{\text{out}} + \gamma_{\text{inel}}$, while the time-independent spectrum is sensitive to the ratio of decay rates $\gamma_{\text{out}}/\gamma_{\text{inel}}$ as well as to the total rate. We find that it is essential to include inelastic decay in the model, since if it is omitted the observed area of the $J = 4$ peak in the time-independent spectrum is too large with respect to the $J = 0$ and $J = 2$ peaks to be consistent with the theory. Including inelastic decay greatly complicates the analysis. The original $l = 4$ shape resonance, involving the external atomic degrees of freedom only, splits into a set of shape resonance states arising from the spin-spin and Zeeman interactions of two atoms, confined to move inside a barrier. The energy eigenvalues and inelastic decay widths can be calculated if we assume that additional shape resonances do not occur for (F, l) combinations different from the combination $(6, 4)$ for the entrance channel. The spin-spin radial transition matrix element then derived is to be considered as an upper limit. The actual value may be much smaller: additional shape resonances with their large number of available decay channels strongly enhance the decay. Information on the singlet potential will be needed to deal with this more general case and thus to shed light on the nature of the largely unexplored indirect part of the spin-spin interaction [12,13]. Figure 2 shows the calculated spectrum of shape resonance states for $B = 0$, split according to the total molecular quantum number $\mathcal{F}$ ($\vec{\mathcal{F}} = \vec{F} + \vec{l}$), and some of the Zeeman split states. The $B = 0$ splitting is given for the special case of the direct (dipolar) spin-spin interaction. A fascinating aspect is the weakness of the coupling between $\vec{F}$ and $\vec{l}$. Taking into account the available volume inside the barrier it is only of order 0.02 mK. The 7 G experimental field is sufficient to break the coupling. Only one radial transition matrix element determines both the spectrum and the spin-spin

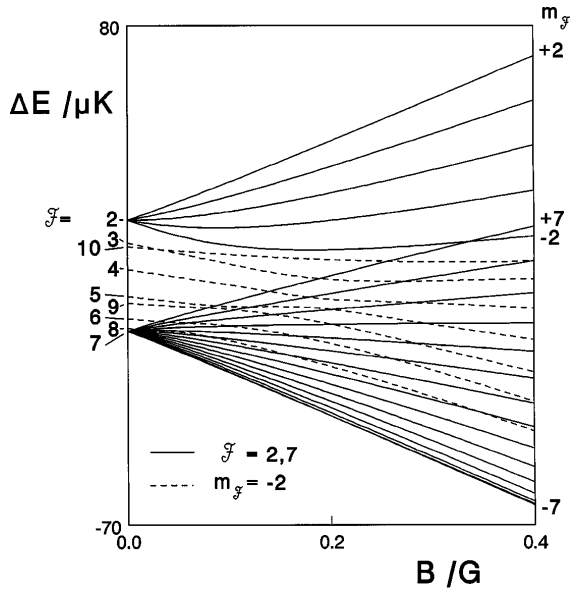

FIG. 2. Spectrum of shape resonance states.

decay widths. We choose γ^0_{inel} for the fully aligned state $\mathcal{F}, m_{\mathcal{F}} = 10, +10$ as a single parameter and find that the theory and the time-independent data are consistent only if $\gamma_{\text{out}}/\gamma^0_{\text{inel}} = 2 \pm 1$. Note that the same $J = 4$ suppression can be achieved with a smaller γ^0_{inel} assuming additional shape resonance states.

In order to simplify the time-dependent analysis, we chose to take the time-dependent data at a sufficiently high laser intensity so that γ_L dominates over the inelastic decay rates during the PA laser pulses. The number of pairs of trapped atoms N_{in} which are in one of the resonance states evolves according to

$$\frac{dN_{\text{in}}}{dt} = -\{\gamma_L + \gamma_{\text{out}} + \gamma_{\text{inel}}\}N_{\text{in}} + \gamma_{\text{in}}N_{\text{out}}\,, \quad (1)$$

$$\frac{dN_{\text{out}}}{dt} = -\gamma_{\text{in}}N_{\text{out}} + \gamma_{\text{out}}N_{\text{in}}\,, \quad (2)$$

where N_{out} is the number of trapped atoms in the entrance channel outside the barrier, and the γ_L term is included only during the photoassociation laser pulses and the γ_{inel} term only in between.

Because of the high laser intensity saturation effects need to be taken into account in γ_L and in the resonance energy E_{res} determining γ_{in} and γ_{out}. We therefore calculated these quantities by means of a two state coupled-channels program with a triplet ground-state channel and a 0^-_g excited-state channel including an absorptive potential accounting for spontaneous emission. Solving the above equations we then calculated the atom loss during the 200 ms period with either one laser pulse or two laser pulses per cycle. An interesting aspect of the theoretical prediction for the difference signal is its asymmetry relative to the $J = 4$ peak itself, which is due to the variation of the tunneling rate over the width of the power-broadened shape resonance. It is also visible in the experimental difference signals. Integrated over the laser detuning and summed over the resonance states, the calculated losses can directly be compared with the corresponding experimental peak areas for a set of delay times and laser intensities. From this we determine the lifetime $\tau = (\gamma_{\text{out}} + \gamma^0_{\text{inel}})^{-1}$ of the aligned shape resonance state for a number of $\gamma_{\text{out}}/\gamma^0_{\text{inel}}$ ratios. Combining this result with time-independent data, we find a value $0.6 < E_{\text{res}} < 0.8$ mK for the resonance energy, well below the barrier height 2.6 mK, a tunneling time $1 < 1/\gamma_{\text{out}} < 4$ μs, and an inelastic decay time $2 < 1/\gamma^0_{\text{inel}} < 8$ μs. Figure 3 shows a typical experimental signal as a function of delay time: A_2/A_1 is the total loss A_2 due to the set of second pulses only (area of $J = 4$ peak in the difference spectrum), divided by the total loss A_1 due to the set of single laser pulses per cycle (area of $J = 4$ peak in case a). Theoretical curves are shown for a set of resonance lifetimes τ. The nonzero ratio at $T = 0$ is due to tunneling during the laser pulses that is somewhat enhanced by the power broadening.

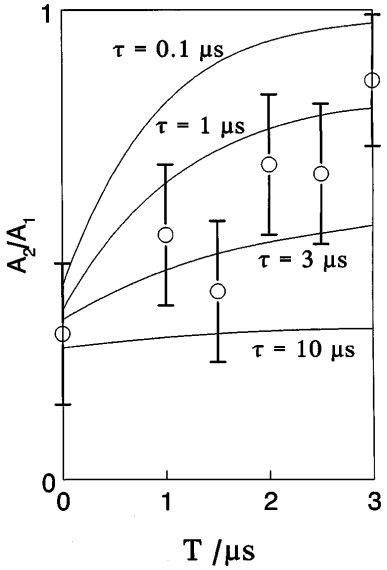

FIG. 3. Time-dependent photoassociation signal A_2/A_1 as a function of delay time T for $I = 50$ W/cm^2, $T = 0.35$ mK, and $\gamma_{\text{out}}/\gamma^0_{\text{inel}} = 2$. Experimental data with error bars are indicated as well as theoretical curves for various lifetimes τ.

The above range of γ^0_{inel} implies an upper limit for the decay rate due to spin-spin relaxation in the s-wave channel, which turns out to be far larger than both the theoretical estimate [13] and the experimental value following from recent experiments with a ^{87}Rb Bose condensate [14]. This suggests that indeed additional shape resonances play a role in our experiment. The E_{res} range is only slightly shifted in this way.

Using this and peak areas of $J = 0, 2$ lines for three subsequent vibrational levels in the time-independent spectrum, we determine an accurate value 4550 ± 100 a.u. for the van der Waals coefficient C_6, in good agreement with a recent theoretical value 4426 a.u. [15]. Finally, with this C_6 value and the above-mentioned resonance energy we determine the triplet scattering length to be in the range $-500a_0 < a_T(^{85}\text{Rb} + ^{85}\text{Rb}) < -300a_0$, narrower than the range $-1000a_0 < a_T < -60a_0$ found in Ref. [10] and obtained with less input of theoretical parameters. The negative sign of a_T implies that a homogeneous ^{85}Rb gas sample will not form a stable condensate.

With additional experiments, we have found that doubly polarized ^{87}Rb atoms exhibit a d-wave shape resonance, the details of which will be reported elsewhere [5]. We use the condition that mass-scaled results of separate ^{85}Rb and ^{87}Rb analyses are consistent to derive the number of bound states n_b in the $^{85}Rb_2$ and $^{87}Rb_2$ triplet ground states. We find $n_b = 38 \pm 1$ for $^{85}Rb_2$ and 39 ± 1 for $^{87}Rb_2$, the latter value being in good agreement with the theoretical value 38 derived in Ref. [16]. To our knowledge, there is no other experimental information on this quantity. The difference in n_b for the two isotopes is connected with the difference in sign of the respective scattering lengths: the state which becomes bound with the increasing atomic mass causes the $^{85}Rb_2$ scattering length to be negative and the $^{87}Rb_2$ scattering length to be positive.

In conclusion, by means of a pulsed photoassociation experiment we have observed the time dependence of a collision of two cold ^{85}Rb atoms via a shape resonance. Combining this observation with time-independent data we have obtained new insight in elastic and inelastic processes, of importance for present and future cold atom experiments.

[1] M. H. Anderson, J. R. Ensher, M. R. Matthews, C. E. Wieman, and E. A. Cornell, Science **269**, 198 (1995).
[2] C. C. Bradley, C. A. Sacket, J. J. Tollet, and R. G. Hulet, Phys. Rev. Lett. **75**, 1687 (1995).
[3] K. B. Davis, M.-O. Mewes, M. R. Anderson, N. J. van Druten, D. S. Durfee, D. M. Kurn, and W. Ketterle, Phys. Rev. Lett. **75**, 3969 (1995).
[4] K. Gibble and S. Chu, Metrologia **29**, 201 (1992).
[5] H. M. J. M. Boesten, C. C. Tsai, J. R. Gardner, D. J. Heinzen, and B. J. Verhaar (unpublished).
[6] J. D. Miller, R. A. Cline, and D. J. Heinzen, Phys. Rev. Lett. **71**, 2204 (1993); R. A. Cline, J. D. Miller, and D. J. Heinzen, Phys. Rev. Lett. **73**, 632 (1994).
[7] L. P. Ratliff, M. E. Wagshull, P. D. Lett, S. L. Rolston, and W. D. Phillips, J. Chem. Phys. **101**, 2638 (1994).
[8] W. I. McAlexander, E. R. I. Abraham, N. W. M. Ritchie, C. J. Williams, H. T. C. Stoof, and R. G. Hulet, Phys. Rev. A **51**, 871 (1995).
[9] R. Napolitano, J. Weiner, C. J. Williams, and P. S. Julienne, Phys. Rev. Lett. **73**, 1352 (1994).
[10] J. R. Gardner, R. A. Cline, J. D. Miller, D. J. Heinzen, H. M. J. M. Boesten, and B. J. Verhaar, Phys. Rev. Lett. **74**, 3764 (1995).
[11] G. Herzberg, *Spectra of Diatomic Molecules* (Van Nostrand Reinhold, New York, 1950), 2nd ed., p. 226; to our knowledge this is the first observed example of a Hund's case (e) structure.
[12] A. M. Mizushima, *The Theory of Rotating Diatomic Molecules* (Wiley & Sons, New York, 1975).
[13] F. H. Mies, C. J. Williams, P. S. Julienne, and M. Krauss (unpublished).
[14] C. Wieman (private communication).
[15] M. Marinescu, H. R. Sadeghpour, and A. Dalgarno, Phys. Rev. A **49**, 982 (1994).
[16] M. Krauss and W. J. Stevens, J. Chem. Phys. **93**, 4236 (1993).